PCCP

Accepted Manuscript

ROYAL SOCIETY OF CHEMISTRY

www.rsc.org/pccp

Electrocatalysis on gold

Paramaconi Rodriguez [a] and Marc T.M. Koper [b]

[a] School of Chemistry, The University of Birmingham, Birmingham B15 2TT, United Kingdom

[b] Leiden Institute of Chemistry, Leiden University, PO Box 9502, 2300 RA Leiden, The Netherlands.

Corresponding authors: p.b.rodriguez@bham.ac.uk, m.koper@chem.leidenuniv.nl

Abstract

This perspective article reviews recent advances in the study of important catalytic reactions on gold electrodes. The paper discusses both oxidation and reduction reactions: the oxidation of carbon monoxide and alcohols as well as the oxygen reduction reaction on gold electrodes and also a brief discussion of other interesting reactions on gold electrodes such as the amine borane oxidation and the CO_2 reduction. A common theme in electrocatalysis on gold is the sensitive dependence of various reaction rates on pH and gold surface structure. The electrocatalysis of redox reactions on gold is highly pH dependent, often preferring alkaline media, due to the prominent role of negatively charged reaction intermediates related to the fact that gold does not bind the neutral intermediates strong enough. Gold also tends to be a selective catalyst, again due to its weak adsorption properties, as on gold the reaction often stops when a difficult bond breaking or making event would be the necessary next step.

1. Introduction

“Gold makes the ugly beautiful” is a quote from Jean-Baptiste Poquelin, better known as Molière, a French theatre writer, director and actor, and considered as one of the masters of comic satire. In catalysis, gold was long considered the “ugly duckling” for being a too noble and therefore catalytically inactive material. However, during the last three decades, the catalytic activity of gold has attracted increasing scientific attention[1-12]. In gas-phase catalysis, most of the work has focused on the catalytic activity of gold nanoparticles supported on different metal oxides [13-18], which were shown by Haruta to have a surprisingly high catalytic activity towards CO oxidation at low temperature[16,19] . Even though well-defined Au surfaces have showed an interesting reactivity toward other reactions in the gas phase [11,20-24], the CO oxidation is catalyzed only by oxide-supported gold nanoparticles. It is well documented that the size and the shape of Au particles, the nature of the support, and the preparation method all play a crucial role in influencing the catalytic activity [8,9,15,17,18,25].

In liquid-phase electrocatalysis, the catalytic activity of bulk gold surfaces in electrochemical environment has been investigated extensively[1,3,4,26-36]. The low overpotential for the oxidation of carbon monoxide on gold electrodes in alkaline media was reported first by Roberts Jr. and Sawyer in 1964 [26,27]. The most significant parameters that influence the catalytic activity of gold in electrochemical media are the surface structure [30-32,34,37] and the electrolyte pH [26,27,29,31,38]. However, the surprisingly high catalytic activity of gold under electrochemical conditions goes beyond the oxidation of carbon monoxide since in alkaline media gold electrodes also show enhanced catalytic activity for the oxidation of alcohols[1,33,39] and for the oxygen reduction reaction (ORR)[40-42]. Contrary to the situation in gas phase catalysis, only few studies in electrocatalysis have considered the effect of the support on the catalytic activity of supported gold nanoparticles. Significantly, a contribution by Hayden et at.[43,44], who studied the catalysis of gold nanoparticles on carbon and conductive titanium oxide electrodes in acidic media, showed that carbon-supported gold nanoparticles show a low activity towards the CO oxidation similar to that of bulk gold in acidic media, in contrast to gold nanoparticles supported on sub-stoichiometric titanium dioxide which showed high activity at low overpotential, comparable to bulk gold in alkaline media.

This paper explores the conditions and properties that make “ugly gold” beautiful under electrochemical conditions, under the assumption that if these properties are better understood, gold may be better exploited for (electro)catalysis. On the basis of the examples collected in this Perspective, we will argue that it is the tunability of gold’s relative catalytic inertness, in combination with the electrolyte pH, that makes it such an interesting catalyst for certain catalytic transformations.

2. The electrochemical oxidation of carbon monoxide on gold electrodes.

The electrochemical CO oxidation on gold has been widely studied. In particular the effect of the surface structure and the effect of the pH on the catalytic activity have attracted the attention of many groups [26,27,29-32,37,38,45,46]. Before discussing the effect of the pH on the adsorption and oxidation of CO on gold electrodes, it is important to realize that a change of pH results not only in a change of the H^+ or OH^- concentration in the electrolyte but also results in an indirect change of the absolute potential range and the electrostatic properties of the electrochemical interface. As the oxidation of CO is a reaction in which an equal number of protons and electrons are transferred (i.e. two), from a thermodynamic point-of-view it makes sense to plot the voltammetry on the pH independent reference scale of the Reversible Hydrogen Electrode (RHE). Moreover, the electrochemical potential window is restricted to the potential range in which water is stable, which is also expected to be independent of potential on the RHE scale. However, on the absolute scale of the standard hydrogen electrode (SHE), a change in pH leads to a change in the absolute potential of 59 mV/pH, and a corresponding change in the local double layer structure and the electric field at the electrode–electrolyte interface. Such an effect may lead to changes in the adsorption strength of carbon monoxide to the (gold) electrode.[47] Therefore, the binding of carbon monoxide to gold in acidic and alkaline solution may not be same, even if they are studied on the same potential on the RHE scale, because the absolute potential on the SHE scale is not the same in the two media. A good example of this effect was measured many years ago by Kunimatsu et al.[48] , who compared the C-O stretching frequency of CO chemisorbed on gold electrodes in acidic and alkaline media, showing that the C-O stretching frequencies obtained in acidic and alkaline solution fall onto a single curve on the SHE scale. This suggests that the electrochemical Stark tuning effect, i.e. the effect of the electrode potential on the vibrational properties of a chemisorbate, can also employed to understand differences between chemisorbates adsorbed on electrode surfaces at different pH.

One example of this pH-induced effect is the CO oxidation reaction. In acidic media, due to the weak adsorption energy of CO on gold, the CO oxidation takes places at high overpotentials [31,38,48,49]. This makes gold a “bad” catalyst toward the CO oxidation in acidic media. However, it has been demonstrated that in alkaline media the catalytic activity of gold towards the CO oxidation is superior to the catalytic activity of a Pt electrode [48,49]. Moreover, we have reported experimental evidence for the irreversible adsorption of CO on gold single-crystal electrodes in alkaline media[32]. Counterintuitively, CO remains chemisorbed on the gold surface in alkaline media, even in the absence of CO in solution, leading to the appearance of an unusual adsorption state of the CO on Au(111) and hexagonally-reconstructed Au(100) electrodes. Figure 1A, curve (a) shows the voltammetric profile of Au(111) in 0.1 M NaOH. The peak at 1.10 V before the onset of the surface oxidation at 1.2 V, is associated with the lifting of the (1×√23) reconstruction of the surface[34]. This lifting of the surface reconstruction is supposed to be induced by the early stages of “irreversible” OH− chemisorption or oxide formation. Curve (b) corresponds to the voltammetric profile of the Au(111) with CO irreversibly adsorbed. In the positive scan, a sharp peak is observed at 0.4 V. When the cyclic scan is limited to the potential region between 0.05 V and 0.5 V (curve 1b), this peak appears as almost reversible. If the upper limit potential is extended, an additional oxidation current is observed between 0.8 and 1.1 V , which is ascribed to the oxidation of adsorbed CO, in agreement with earlier observations[49]. Figure 1c shows the voltammetry of the continuous oxidation of carbon monoxide on Au(111), i.e. with CO in solution. Most likely, the voltammetric feature at 0.4 V is associated with the co-adsorption (and desorption) of hydroxide from the alkaline solution at low potentials, in view of its marked pH-dependence [31,32]. As was reported previously[31,37], in acidic media, the CO oxidation on gold takes place at much higher overpotentials (see figure 1B, which the continuous oxidation of CO on Au in acidic and alkaline media), and CO does not remain chemisorbed on the gold surface in the absence of CO in solution. The higher catalytic activity in alkaline media was attributed to CO chemisorption and an associated “self-promotion mechanism” [29,31]. In this mechanism, CO and OH enhance each other’s bonding to the Au(111) surface in alkaline media. This leads to a higher coverage of OH on the surface than in the absence of CO, and this adsorbed OH is active in the oxidation of solution-phase CO:

$$CO_{sol} + OH_{ads} \rightarrow CO_2 + H^+ + e^- \qquad (1)$$

The solution-phase CO_{sol} may in fact be in a (weakly) adsorbed state when it reacts with OH_{ads}, very much like in a Langmuir-Hinshelwood reaction.

Density Functional Theory calculations indeed predict that CO chemisorbed to Au(111) enhances the nearby bonding of OH to the surface, through what appears to be a local gold-mediated donation-back donation mechanism driven by a change in the local electrostatics[29,30]. Electroreflectance measurements performed by Cuesta et al.[38] also confirm that CO chemisorption on gold takes place only if a filled high-energy surface state takes part in the chemisorption bond. The threshold potential to fill this high-energy surface state is only achievable in alkaline media.

Hayden et al.[43,44] prepared thin conductive titania electrodes in order to study the effect of the support towards the CO oxidation on supported gold nanoparticles. They found that, contrary to the observed low activity of bulk gold electrodes in acidic media, gold nanoparticles between 2-7 nm supported on sub-stoichiometric titanium dioxide showed high activity towards the oxidation of CO in acidic media with low overpotential (figure 2). The highest enhancement was observed for nanoparticle with 3 nm diameter over the sub-stoichiometric titanium dioxide. We recently confirmed the results presented by Hayden et al.[43,44], and in addition we showed that the enhancement in the CO oxidation in acidic media is also observed when TiO_2, TiO_x and MgO nanoparticles are supported on Au polycrystalline electrode[50]. These new results suggest that electronic interaction between the gold and the metal oxide are the driving force behind the enhanced catalytic activity of CO oxidation in acidic media, an activity which is comparable to the activity observed in alkaline media. We have proposed that the electronic interaction of the oxide with gold yields more electron-rich Au particles. Such charge redistribution in the Au/oxide system would shift the Fermi level of gold, such that the absolute potential of gold would mimic the conditions in alkaline media. As a result, the electronic interaction of gold with the oxide gives rise to the conditions similar to the “self-promotion mechanism” of the CO electrochemical oxidation on gold in alkaline media[29,31]. For this model to be fully confirmed, more detailed spectroscopic experiments will be necessary in the future, primarily aimed at probing the electronic structure of gold under different conditions.

3. Electrochemical oxidation of alcohols and sugars on gold

The electrochemical oxidation of small alcohols has been widely studied because of their possible use in fuel cells. Since the development of the proton exchange membrane (PEM) as the electrolyte for fuel cells, the oxidation of alcohols such as methanol, ethanol, 2-propanol, ethylene glycol and glycerol in acidic media has been considered for fuel cell applications[33,51-55]. In direct alcohol fuel cells (DAFCs), the alcohol is directly oxidised at the anode, ideally through a complete oxidation pathway to CO_2. The oxidation of alcohols on gold electrodes in acidic media typically shows very low activity, whilst in alkaline media gold is substantially more active for alcohol oxidation, and can even surpass platinum in terms of total oxidation current. This makes alcohols interesting fuels for future low-temperature fuel cells based on alkaline membrane technology, and gold an interesting catalyst for such applications.

The enhanced oxidation of small alcohols, such as methanol, ethanol and glycerol on gold electrodes in alkaline media has been attributed to the deprotonation of the R-OH group at sufficiently high pH, leading to the formation of the alkoxide species (RO^-). The alkoxide species is much more active in oxidation reactions[39]. To illustrate this effect Fig 3A shows how the peak current density of the ethanol oxidation on a gold electrode increases rapidly with pH [56]. It is proposed that at a pH higher than ca. 11, the ethoxy anion is the main reactive species and since its equilibrium concentration steeply increases with pH, so does the overall oxidation activity [39,56]. The first oxidation product is acetaldehyde. A similar pH effect has also been observed for other alcohols. Therefore, alcohol deprotonation is the key first step for alcohol oxidation in alkaline media:

$$R\text{-}OH \leftrightarrows R\text{-}O^- + H^+ \qquad (2)$$

with the further oxidation of R-O^- to the corresponding aldehyde being rate determining. Since the pK_a of reaction (2) depends on the nature of R, alcohols with a lower pK_a, such as the sugar alcohols or glycerol, have a high oxidation activity, whereas alcohols with a high pK_a (such as isopropanol and isobutanol), are significantly less active at pH = 11. This Hammond relationship between oxidation activity and pK_a is confirmed in Figure 3B which shows an approximately linear relation between the onset potential for the oxidation of various alcohols and the pK_a of the corresponding alcohol. For this relationship to hold, it is important that the variation in the reactivity of R is small.

The electrochemical oxidation of glycerol is a reaction that has recently been studied extensively on gold electrodes [33,57,58]. Glycerol can be used as fuel in a fuel cell device but is also used in pharmaceutical formulations and in the manufacture of cosmetics. Kwon et al. have studied the pH dependence of the activity and product selectivity of glycerol oxidation on gold (and platinum) using online HPLC[33]. At pH=13, the main oxidation products are glycolic acid and formic acid (in equal amounts) and a smaller amount of glyceric acid, which is the precursor to glycolic acid and formic acid. In neutral media, only glyceraldehyde was observed, suggesting that in alkaline media, glyceraldehyde is the precursor for the formation of glyceric acid. No products were observed from glycerol oxidation on gold in acidic media. Fernandes Gomes et al.[58] also reported on the effect of the pH in the oxidation of glycerol on gold electrodes and identified from in situ infrared spectroscopy dihydroxyacetone, tartronic acid, mesoxalic acid, glyoxylic acid, and carbon dioxide as products in alkaline media, whereas in acidic medium tartronic acid, formic acid, and carbon dioxide were observed. In the HPLC study [33], these products were only observed on platinum electrodes. One striking observation concerns the comparison between the catalytic activity of Au and Pt for glycerol oxidation in alkaline media. Whereas on Pt the onset potential for glycerol oxidation is lower, at high anodic potential (ca. 1.2 V vs RHE), gold exhibits the higher current density. The main reason for this is the lower propensity of gold to form surface oxides, which inhibit the alcohol oxidation activity. Therefore, while Pt is an intrinsically better catalyst, with a lower overpotential and the capability to oxidize alcohols completely to CO_2 (at least to some extent), gold can achieve higher turn-over rates at sufficiently high overpotential due its lower reactivity towards water and the absence of CO poisoning. Therefore, the high activity of gold for the oxidation of alcohols in alkaline media has little to do with any special catalytic property of gold, but rather with the favourable reaction conditions in solution combined with low tendency of gold to become poisoned by either CO or surface oxides.

In addition to the oxidation of small alcohols, the electrochemical oxidation of a wide range of sugar alcohols (i.e., D-glucose, xylose, etc.) has been studied on polycrystalline gold electrodes [59-62]. Such studies are of interest because gold is extensively used as electrodes in the electrochemical detection of sugar concentration in blood [61-63]. Such studies focus on the sensitivity of the detection [61-63] and the product selectivity [60]. Kokoh et al. report that gold electrodes are more active, and therefore more sensitive, towards the oxidation of D-glucose than platinum [64]. Rao et al. suggest that this is due to the fact that glucose oxidation leads to gluconic acid, in neutral and acidic media; this product accumulates in the bulk and inhibits the further oxidation of glucose [65]. As with the oxidation of CO and smaller alcohols, the reactivity of glucose and other sugars has been observed to be much higher in alkaline medium [66]. Gold also displays a higher catalytic activity for the oxidation of d-xylose than Pt. The lower activity of Pt is again due to oxide formation and CO poisoning on Pt [67].

In addition to the pH effect, the surface structure also affects the reactivity of gold electrodes for alcohol oxidation [68-70]. Figure 4 shows the activity of the three gold basal planes towards the oxidation of ethanol (Fig.4A) and ethylene glycol (Fig. 4B) in alkaline media. As can be seen in both figures, even though the onset of oxidation is similar for the three basal planes, the catalytic activity of the Au(111) electrode at high potentials is significantly higher than on Au(100), whereas the Au(110) shows the lowest activity. The simplest explanation for this observation refers to the propensity of the different surfaces to form surface oxides. The Au(110) surface is oxidized the easiest, and is therefore much less active for alcohol oxidation than Au(111), which has a much higher surface oxidation potential.

In a recent paper, we have applied our model for CO oxidation on gold in alkaline media (section 2) to the oxidation of alcohols [3]. We demonstrated that in strong contrast to transition-metal electrocatalysis, for which CO has always been considered a poison, adsorbed CO on Au can act as a promoter for the oxidation of certain alcohols, in particular methanol. The idea is that adsorbed CO enhances the adsorption of OH, and this adsorbed OH helps the deprotonation of the alcohol to the corresponding aldehyde. Figure 5A compares the voltammetry of a 0.1 M methanol solution in 0.1 M NaOH on a “clean” Au(111) electrode to the same methanol oxidation reaction on a Au(111) electrode modified with irreversibly adsorbed CO. On the unmodified Au(111) in alkaline media the onset of the oxidation of methanol is at ca. 1.0 V. On the Au(111)-CO electrode, however, an oxidation current is observed at significantly lower potential. By using online HPLC (Figure 5B and 5C) and in situ FTIR, it was confirmed that this current is due to the oxidation of methanol, which is shifted to lower potentials and superimposed on the sharp feature at 0.4 V. Figure 5 clearly shows that on the Au(111)-CO electrode, the formation of formaldehyde is enhanced and shifted by ca. 0.5 V compared to unmodified Au(111). Clearly, the adsorbed CO must act as a promoter for methanol oxidation on Au(111). It is interesting to point out that in alkaline media the electrochemical oxidation of methanol on a Pt(111) electrode surface starts at around 0.7 V vs RHE [71], a potential related to the onset of the oxidation of strongly adsorbed CO. The electrochemical oxidation of methanol on a CO-modified

Au(111) electrode starts at a lower potential [3]. We also note that this promoting effect is sensitive to the gold surface structure. The CO promotion effect has only been observed on Au(111) and on the hexagonally reconstructed Au(100) surface. Recent Density Functional Theory (DFT) calculations [72] suggest that this is an electronic effect: adsorbed CO leads to a significant lowering of the work function of gold only on the Au(111) surface. This lowering of the work function helps the electron transfer needed to bind the electronegative OH adsorbate.

The electrochemical oxidation of alcohols has been studied on Au nanoparticles prepared by different synthesis methods[73-80] . Even though some of these studies include the effect of the electrolyte composition and shape of the nanoparticles, to our knowledge there is no detailed study on the influence of the particle size and shape and the effect of the support on the activity for alcohol oxidation.

The special activity of gold nanoparticles has also been studied in the field of liquid-phase heterogeneous catalysis [81]. In such experiments, the alcohol is oxidized in an aqueous (typically alkaline) solution of gold nanoparticles using oxygen as an oxidizing agent. The role of oxygen here is primarily to impose a potential to the gold-electrolyte interface at which the alcohol oxidation can take place electrochemically. This role of oxygen as a depolarizing agent rather than as an oxygen transfer agent, was confirmed by isotope-labelling experiments [82]. Therefore, the oxidation of alcohols under such conditions appears to be not essentially different from electrochemical oxidation. The only possible additional effect is any direct influence of the presence of oxygen, for instance through the formation of hydrogen peroxide, which is the main product of oxygen reduction at the gold-electrolyte interface (for a detailed discussion, see next section). Hydrogen peroxide has been suggested as a powerful oxidant in gold-catalyzed alcohol oxidation[83,84]. This potential role of hydrogen peroxide has been studied electrochemically by assessing the electrochemical activity of glycerol oxidation at gold in alkaline media in the absence and presence of oxygen or hydrogen peroxide [85]. These studies revealed that the presence of hydrogen peroxide does not lead to any significant modification of the rate or products of electrochemical oxidation, and therefore hydrogen peroxide has no major influence on the rate or the pathway of alcohol oxidation on gold in the aqueous phase.

4. The Oxygen reduction reaction.

An important electrocatalytic reaction that has been extensively studied on gold electrodes is the oxygen reduction reaction (ORR) [41,42,86-88]. The mechanism for ORR includes several individual steps and two main pathways mechanism are normally considered. One pathway involves the formation of water through the transfer of four protons and electrons, and the other pathway produces hydrogen peroxide through a two-proton-electron pathway [89]. It is likely that these pathways are not actually independent, but that the four-electron transfer pathway proceeds through an (adsorbed) hydrogen peroxide-type intermediate. A successful ORR fuel cell catalyst would reduce oxygen molecules to water through the four-electron route with a low overpotential. Incomplete reduction of oxygen to hydrogen peroxide leads to a low energy conversion efficiency. On the other hand, the selective formation of hydrogen peroxide could be of interest from the synthetic point-of-view.

Experiments show a remarkable influence of the pH and of the crystallographic orientation on the kinetics and the mechanism of the ORR on Au electrodes [41,90-94]. The ORR on Au has a higher rate in alkaline media than in acidic media, a feature that is common for all electrode surfaces that interact weakly with oxygen (i.e. Ag, C, and Hg). The Au(111) electrode was found to have the lowest activity towards the ORR among the three basal planes of gold, both in acidic and alkaline media, while the most active surface is Au(100)

(Figure 6). Most interestingly, in alkaline media Au(100) electrodes follow a complete 4e transfer pathway in a certain potential window, while a $2e^-$ process takes place on the Au(111) and Au(110) face. Also, the introduction of steps into the Au(100) surface lowers its ability to complete the $4e^-$ reduction (see Figure 6).

The main features of the pH dependence of the ORR on Au electrodes (as well as on Ag, C and Hg electrodes) can be understood on the basis of the Pourbaix diagram shown in Figure 7, and the assumption that the first and rate-determining step in the mechanism of the ORR on Au is:

$$O_2 + e^- \rightarrow O_2^-(ads) \tag{3}$$

where the O_2^- is either in solution or (weakly) adsorbed on the gold surface. In acidic media, the equilibrium potential of this reaction (-0.31 V vs SHE) is very far from the overall equilibrium potential for the 2 or $4e^-$ transfer (see Figure 7) and hence the reaction is slow. In alkaline media, on the other hand, this difference is much smaller, and potential for the formation of the superoxide anion is closer to the overall equilibrium potential. This is the main reason why electrode materials that interact weakly with oxygen species, such as gold, are such good ORR catalysts in alkaline media [95], though their catalytic interaction is often too weak to lead to O-O bond breaking, making hydrogen peroxide HO_2^- the final product. Figure 8 shows the voltammetry of ORR on polycrystalline gold for various pH values, plotted on both the Standard Hydrogen Electrode Scale (SHE) and the Reversible Hydrogen Electrode scale (RHE), illustrating how with increasing pH the onset potential for ORR shifts closer to the overall thermodynamic potential [96]. This explanation of the pH dependence of the ORR on Au is similar to recent calculations performed by Quaino et al.[97]. They suggested that in acidic media the *d*-band centre and the strong interaction with the intermediates plays an important role in the ORR, while in alkaline media the *d*-band plays no role and the catalytic activity is mainly due to the weak interaction of the O_2^- intermediate and the low coverage of adsorbed OH in the region where oxygen reduction takes place. We also note that computations that assume the same reaction mechanism for the ORR on Pt and Au, such as the one by Viswanathan et al. [98], cannot reproduce the different pH dependences of the overall ORR rate between Pt and Au, as such a mechanism does not include the role of the O_2^- intermediate.

Studies performed by Adzic's group on ORR on stepped Au surfaces show that the catalytic activity for the 4-electron pathway in alkaline solutions is fully associated to the presence of (100) domains[40,92,99], as illustrated in Figure 6. In spite of a number of DFT calculations which have attempted to understand this peculiar structure sensitivity [100,101], the origin of the high catalytic activity of these domains for the ORR is not fully understood. Adzic et al. have suggested that the difference is related to the OH adsorption energy on the (100) domains[40,91,92,94]. However, we note that the specific activity of (100) terraces for bond making and bond breaking is a rather common observation in electrocatalysis [102]. For the oxidation of dimethylether on Pt(100), the activity of the (100) surface has been shown to be related to an active "ensemble" site consisting of four surface atoms in a square arrangement [103], and it is likely that this is also the active site for the ORR on Au(100).

The remarkable structure sensitivity of the ORR on Au in alkaline media translates into a corresponding dependence of the ORR activity on the shape of Au nanoparticle catalysts. Hernandez et al.[88,104-106] used the rotating ring disk electrode (RRDE) to study the electrocatalytic activity and mechanism of the ORR on gold nanoparticles with different size and surface orientation. As shown in Figure 9A, the onset potential for the ORR on cubic nanoparticles is close to the onset potential of the oxygen reduction on Au(100) single crystal electrodes, while the activity of the nanorods is significantly lower than that of the cubic and spherical nanoparticles[88,104,106]. As can be seen in Figure 9B and 9C the formation of H_2O_2

and the total number of electrons transferred per O_2 also differ between the different nanoparticles, the cubic nanoparticles being the most active for the 4-electron reduction, in agreement with the single-crystal results.

The effect of the support and the particle size of gold nanoparticles towards the oxygen reduction reaction have also been subject of study. Gold nanoparticles with particle sizes from 1 nm to 30 nm prepared on highly oriented pyrolytic graphite (HOPG) and boron-doped epitaxial 100-oriented diamond, were investigated for their ORR activity[107]. A dependence of the kinetic currents on the particle size was observed but no effect of the different carbon supports on electrocatalytic activity was found. On the other hand, a strong support effect was observed by Guerin et al.[86] when comparing the catalytic activity of gold nanoparticles on carbon and non-stoichimetric TiO_x supports. The gold nanoparticles supported on non-stoichiometric TiO_x showed a 3 times higher specific activity than nanoparticles deposited on a carbon support. Guerin et al also reported that, independent of the support, nanoparticles with a 3 nm diameter showed the highest specific catalytic activity for ORR and the activity decays rapidly for particle sizes below 3.0 nm. Interestingly, while the ORR seems to be enhanced on small particles (≈ 3nm), Au particles with a diameter below 2.5 nm are less active for oxygen reduction, independent of the supporting material.[86] In agreement with the results of Guerin et al [86], Tang et al. also reported a strong Au nanoparticle size dependence of the ORR kinetics in alkaline media, observing that the ORR kinetic current density (j_{kin}) of the 3 nm gold nanoparticles was 2.5 times higher than that obtained with the 7 nm gold nanoparticles.

Summarizing, the ORR activity on gold electrodes is highest in alkaline media, as a result of a rate-determining step that does not involve proton transfer (reaction 3). The ability of gold to complete the four-electron transfer depends sensitively on the gold surface structure, in particular on the presence of two-dimensional (100) domains. Therefore, cubic

Au nanoparticles in alkaline media exhibit the highest activity. The optimal size of the nanoparticles appears to be close to 3 nm, though these nanoparticles will typically not possess extensive (100) terraces, and therefore HO_2^- will be the main product. The detailed effect of the support is still not so clear and not well understood.

5. Other reactions.

The study of the electrochemical oxidation of borohydride and amine boranes (DMAB) has attracted attention because of their direct use in fuel cells for powering portable electronic devices, mainly due to their high energy density related to the number of electrons transferred per borohydride ion [4,35,36,108-110].

Even though the borohydride oxidation reaction (BOR) involves eight electrons per BH_4^- species (eq.4 below) most of the electrode materials used for this reaction, i.e Ni-, Pd-, and Pt-based electrocatalysts, usually show faradaic efficiencies below 100% [111-113]. In particular, Pt electrodes show efficiencies in the range of 25–75%. This is due the competition between the BH_4^- direct oxidation and the unwanted heterogeneous hydrolysis of the borohydride promoted by Pt. During the heterogeneous hydrolysis, a significant amount of hydrogen is produced (Eq. 5), and the diffusion of the H_2 away from the electrode surface without further oxidation causes the decrease of the faraday efficiency.

$$BH_4^- + 8OH^- \rightarrow BO_2^- + 6H_2O + 8e^- \qquad (4)$$

$$BH_4^- + xOH^- \rightarrow BO_2^- + (x-2)H_2O + (4 - 0.5x)H_2 + xe^- \qquad (5)$$

Interestingly, it has been suggested that the poor catalytic activity of gold electrodes towards the hydrolysis of the BH_4^- makes gold an efficient catalyst for the oxidation of borohydride and amine boranes [4,114]. Still, a recent study from Chatenet et al.[108,115] showed a small but non-negligible generation of H_2 on Au in the BOR potential window. The authors reported that the potential for a sufficient efficiency in the oxidation of BH_4^- (0.5 V vs RHE) is not suitable for fuel conversion in the direct borohydride fuel cell[115]. On the other hand, the oxidation of amine boranes in alkaline media on gold electrodes shows negligible hydrolysis, low oxidation overpotential and high faradic efficiency. In this regard, the study of the oxidation of amine boranes on gold electrodes is important for the development of fuel cell technology based on the use of this compound as a fuel. Plana et al.[35,36] reported a marked difference in the electrochemical oxidation of dimethyl borane on the structure of the gold surface. As shown in figure 10, the onset potential for the initial oxidation increases in the series: Au(110) < Au(111)< Au(100), although the limiting current is ca. 30% higher on Au(100) compared to the other surfaces.

Another reduction reaction that has been studied quite extensively on gold, in addition to the oxygen reduction reaction discussed in section 3, is the electrocatalytic reduction of carbon dioxide. Gold is a rather unique electrode material for CO_2 reduction as it shows the highest activity and faradaic efficiency towards the selective formation of CO, amongst a variety of electrode materials studied for this reaction [116]. Given the unique ability of gold to oxidize CO to CO_2, (see section 2) and the expected catalytic reversibility of two-electron transfer reactions [117], the outstanding activity of gold towards CO_2 reduction to CO is perhaps not that surprising. As a result, this reaction has recently regained quite a bit of attention in relation to the electrochemical mitigation and utilization of CO_2 [118,119]. In agreement with most other electrochemical reactions catalyzed by gold, also the CO_2 reduction on gold is sensitive to pH [120]. From measurements of the pH dependence, the Tafel slope and the CO_2 reaction order on polycrystalline gold, Noda et al.[120] concluded that the rate-determining step is the formation of an adsorbed $CO_2^{\bullet -}$ intermediate. Note the similarity with the rate-determining step for the ORR on gold, which also does not involve a proton transfer, and which involves the formation of a (presumably weakly adsorbed) radical anion. Detailed experimental studies on the structure sensitivity of the CO_2 reduction on Au are not available, although based on DFT calculations, Zhu et al.[119] have suggested that step sites in the gold surface are the most active for this reaction.

5. Concluding remarks

In this Perspective article, we have reviewed the electrocatalysis of a number of important redox reactions on gold electrodes. We believe that from a comparison of these reactions, we can identify a number of recurrent themes. First of all, the electrocatalysis of redox reactions on gold is typically highly pH dependent, often preferring alkaline media. Such pH dependence is usually a sign of decoupled proton-electron transfer steps in the mechanism of the catalytic reaction under study [95]. The intermediates in such a mechanism are often stabilized by their interaction with the solution, implying that the interaction with the “catalytic” gold is weak. Electrocatalysis on gold often favours alkaline media as those conditions favour the adsorption of OH on gold (for CO oxidation) or the stabilization of negatively charged intermediates (for alcohol oxidation, oxygen reduction, perhaps also carbon dioxide reduction). Gold can efficiently perform electron transfer but interacts weakly with reactants and intermediates so that it does not easily poison. This statement holds especially for oxidation reactions, for which the low propensity of gold to form surface oxides is especially advantageous. We have speculated [50] that a possible role of the support, such as that reported for CO oxidation, may be related to a similar electronic effect as that induced by alkaline media, namely that the absolute electrode potential is effectively more negative, promoting the adsorption of reactive species. Secondly, gold tends to be a selective catalyst, again due to its weak adsorption properties. Difficult steps in a mechanism, such as bond breaking or bond making steps, are not easily catalyzed by gold, unless these steps are clearly favoured by thermodynamics. Perhaps “partial” oxidation or reduction is a better term in this respect than “selective”. Thirdly, the catalytic properties of gold may be structure sensitive, as the activity for certain reactions is sensitive to the surface facet studied in single-crystal experiments. The Au(111) surface seems to be preferred when a high oxidation activity is required, due to the weak interaction of this surface with poisoning surface oxides, and the Au(100) surface appears optimal when a bond breaking step is involved. Therefore, with a suitable tuning of the gold surface structure and the electrolyte pH, gold can indeed be a beautiful catalyst for electrochemical reactions.

6. Acknowledgments

P.R. and M.T.M.K acknowledge financial support from the Netherlands Organization for Scientific Research (NWO) through VENI and VICI grants, respectively, and the European Commission (through FP7 Initial Training Network “ELCAT”, Grant Agreement No. 214936-2).

Figure Caption

Figure 1. (A) Voltammetric profiles at 50 mV s^{-1} of the Au(1 1 1) electrode in 0.1 M NaOH (a) in absence of CO, (b) in presence of chemisorbed CO and (c) in presence of CO in solution. Copyright from [32] (B) Hanging-meniscus rotating disk electrodes voltammograms of Au(111) in CO-saturated 0.1 M $HClO_4$ (black) and in CO-saturated 0.1 M NaOH (red) Scan rate: 50 mV s^{-1}. Rotation rate: 1100 rpm.

Figure 2. Comparison of the cyclic voltammetry in CO-saturated 0.5 M $HClO_4$ electrolyte of gold supported on carbon (gray) and titania (black) for four different particle sizes (indicated). Scan rate: 50 mV/s; T=298 K. Reproduced with copyright permission from [44]

Figure 3. (A) Measured current j_p for 0.5 M ethanol oxidation on a gold electrode at peak potential (black curve) or at 1.2 V vs RHE (red curve) minus the background current j_0 as a function of the electrolyte pH using 0.1 M phosphate buffers. (B) Plot of the onset potential of the oxidation versus of various alcohols vs. their pK_a; the alcohols are in order of increasing pK_a: sorbitol, erythritol, glycerol, ethylene glycol, ethanol, iso-propanol, iso-butanol. Reproduced with copyright permission from [39,56]

Figure 4. (A) Voltammetric profile of the (—)Au(111), (—)Au(100), (—)Au(110) and (—) Au(polyoriented) electrodes in (A) 0.1 M NaOH + 0.5 M ethanol . (B) Oxidation of 0.1 M ethylene glycol on Au single crystal electrodes in 0.1 M NaOH. Scan rate: 50 mV/s. Reproduced with copyright permission from [68]

Figure 5. (A) Voltammetric profile of Au(111) in 0.1 M NaOH + 2.5 M CH_3OH in the absence (black curve) and presence (red curve) of adsorbed CO, at a scan rate of 1 mV s^{-1}. b,c, Intensities of the peaks related to the retention times of formaldehyde (B) and formate (C) in the HPLC column as a function of potential. Red open circles: with CO on the Au(111) surface; black solid squares: clean Au(111) surface without CO_{ads}. Data points in B and C are single-point measurements converted into corresponding concentrations by a calibration line with an error smaller than 0.1%. Reproduced with copyright permission from [3]

Figure 6. Disk current densities at 1600 rpm for ORR on the low-index planes of gold as indicated in the figure in 0.1 M NaOH. Reproduced with copyright permission from [91].

Figure 7. Schematic Pourbaix diagram of the relevant reactions for the oxygen reduction on gold.

Figure 8. Voltammetry of oxygen reduction at a polycrystalline gold rotating disk electrode as a function of pH in the absence of buffering anions. (A) voltammetric curves plotted vs the SHE reference; (B) voltammetric curves plotted vs the RHE reference. Rotation rate 2500 rpm, scan rate 10 mV/s. Reproduced with copyright permission from ref 93.

Figure 9. (A) Disk currents on the gold nanorods (solid line), seed nanoparticles (dashed line) and nanocubes (dotted line) in an oxygen saturated 0.1 M NaOH solution at 3500 rpm. (B) Ring currents recorded on the platinum ring at 1 V versus the disk potential. (C) Apparent number of electrons transferred for the oxygen reduction reaction on the gold nanoparticles. Reproduced with copyright permission from [106]

Figure 10. Cyclic voltammograms of Au(1 0 0), Au(1 1 0) and Au(1 1 1) surfaces in 0.1 M KOH in the absence (dotted lines) and presence of 2.0 mM DMAB. Scan rate = 50 mVs^{-1}. The blank voltammograms were multiplied by a factor of ten to allow comparison. Reproduced with copyright permission from [36]

Figures

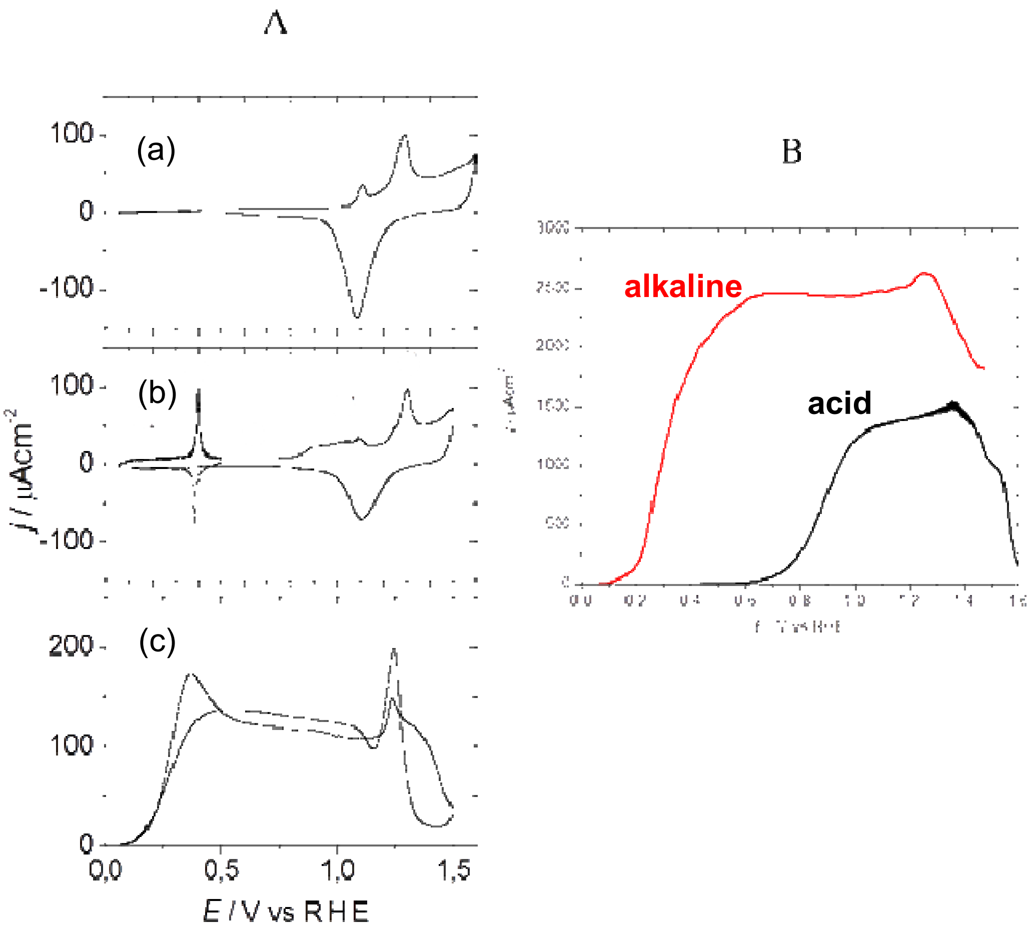
A
(a)
(b)
(c)
100
0
-100
200
j / μAcm^{-2}
0,0
0,5
1,0
1,5
E / V vs RHE
B
alkaline
acid
3000
2500
2000
1500
1000
500
0
0.0
0.2
0.4
0.6
0.8
1.0
1.2
1.4
1.6

Figure 1.

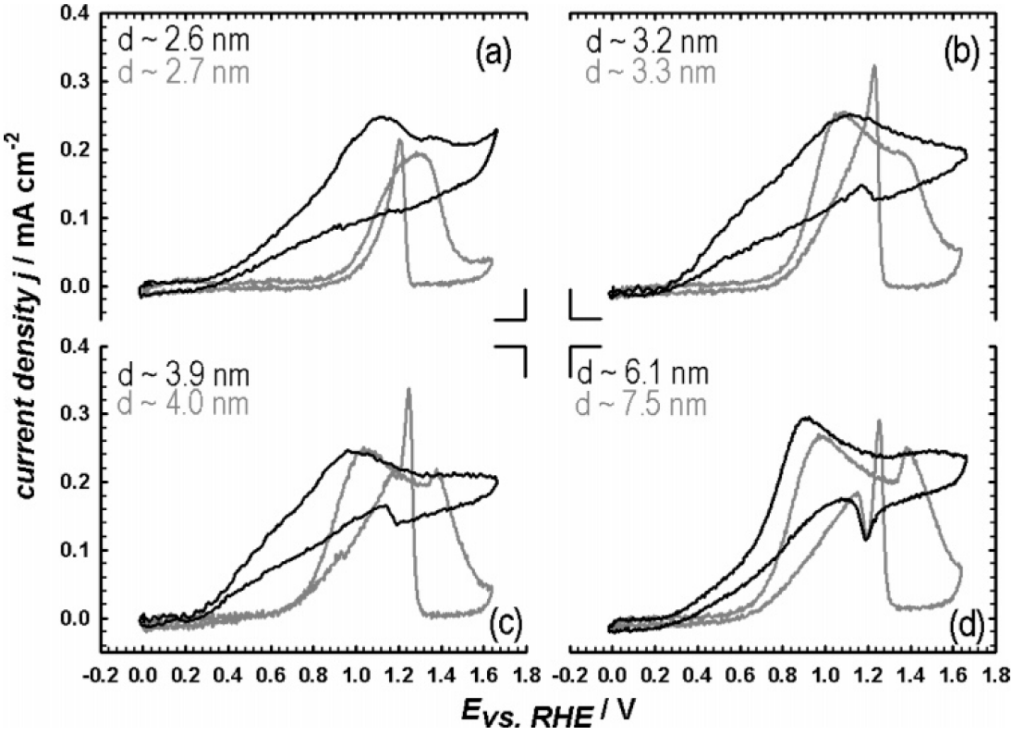
d ~ 2.6 nm
d ~ 2.7 nm
(a)
d ~ 3.2 nm
d ~ 3.3 nm
(b)
d ~ 3.9 nm
d ~ 4.0 nm
(c)
d ~ 6.1 nm
d ~ 7.5 nm
(d)
current density j / mA cm^{-2}
0.4
0.3
0.2
0.1
0.0
-0.2 0.0 0.2 0.4 0.6 0.8 1.0 1.2 1.4 1.6 1.8
$E_{vs. RHE}$ / V

Figure 2.

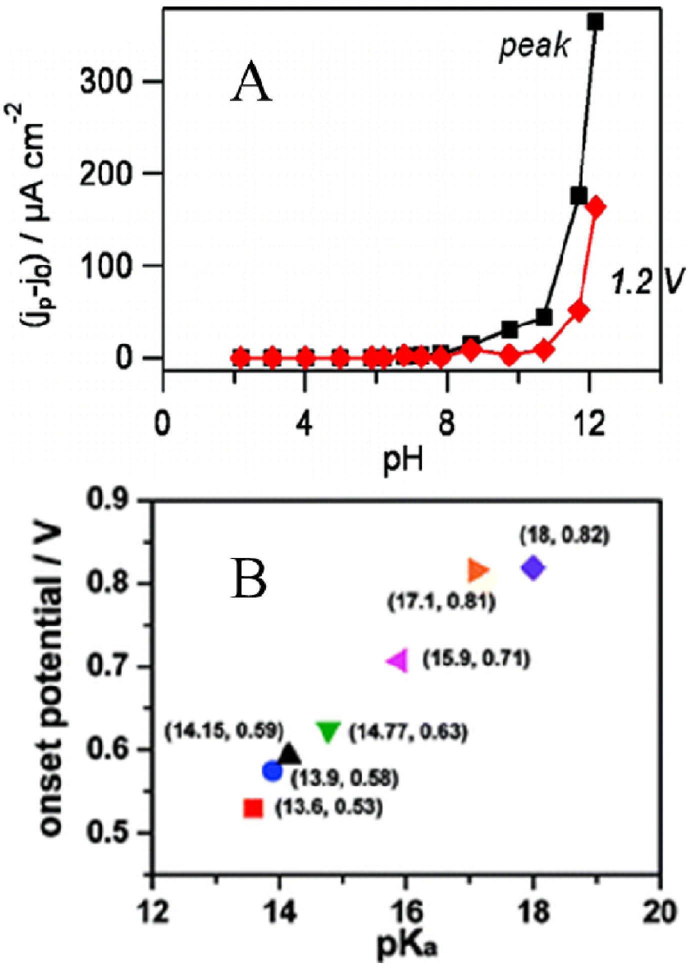
A
peak
1.2 V
(j_p-j_0) / μA cm^{-2}
300
200
100
0
0
4
8
12
pH
B
onset potential / V
0.9
0.8
0.7
0.6
0.5
(18, 0.82)
(17.1, 0.81)
(15.9, 0.71)
(14.15, 0.59)
(14.77, 0.63)
(13.9, 0.58)
(13.6, 0.53)
12
14
16
18
20
pKa

Figure 3.

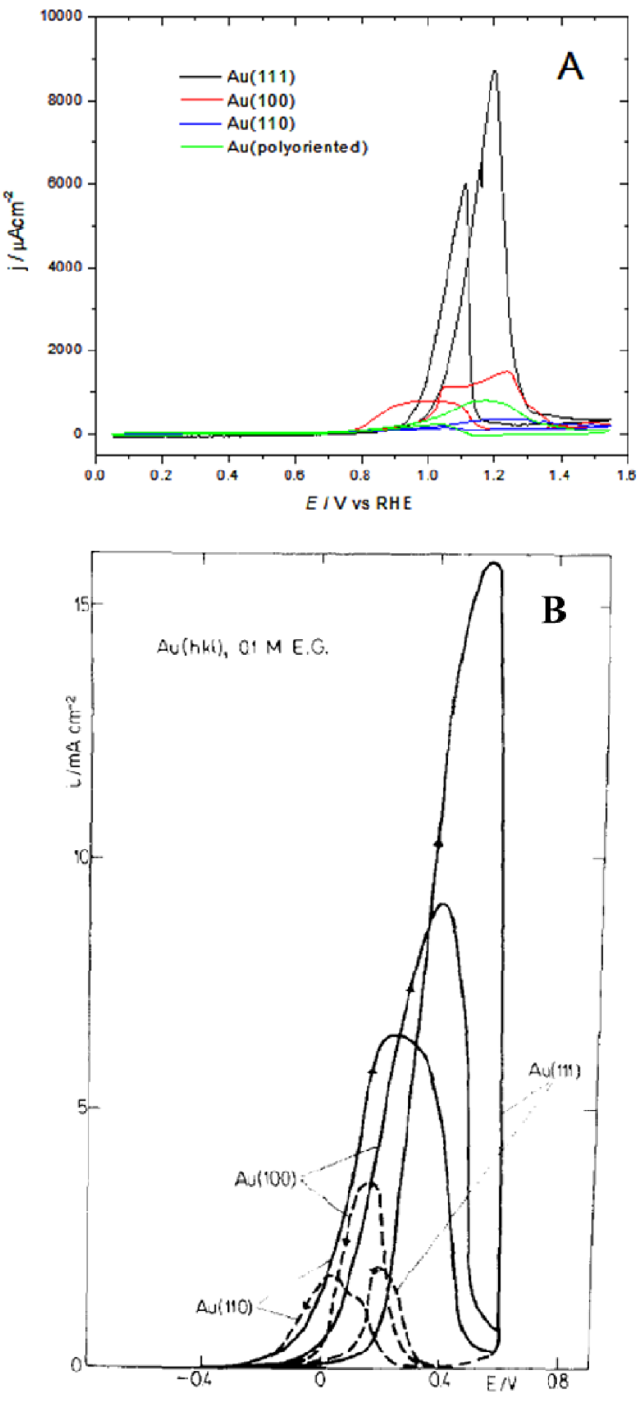
A
Au(111)
Au(100)
Au(110)
Au(polyoriented)
j / μAcm-2
10000
8000
6000
4000
2000
0
0.0
0.2
0.4
0.6
0.8
1.0
1.2
1.4
1.6
E / V vs RHE
B
Au(hkl), 01 M E.G.
ι/mA cm-2
15
10
5
0
Au(111)
Au(100)
Au(110)
−04
0
04
E/V
08

Figure 4

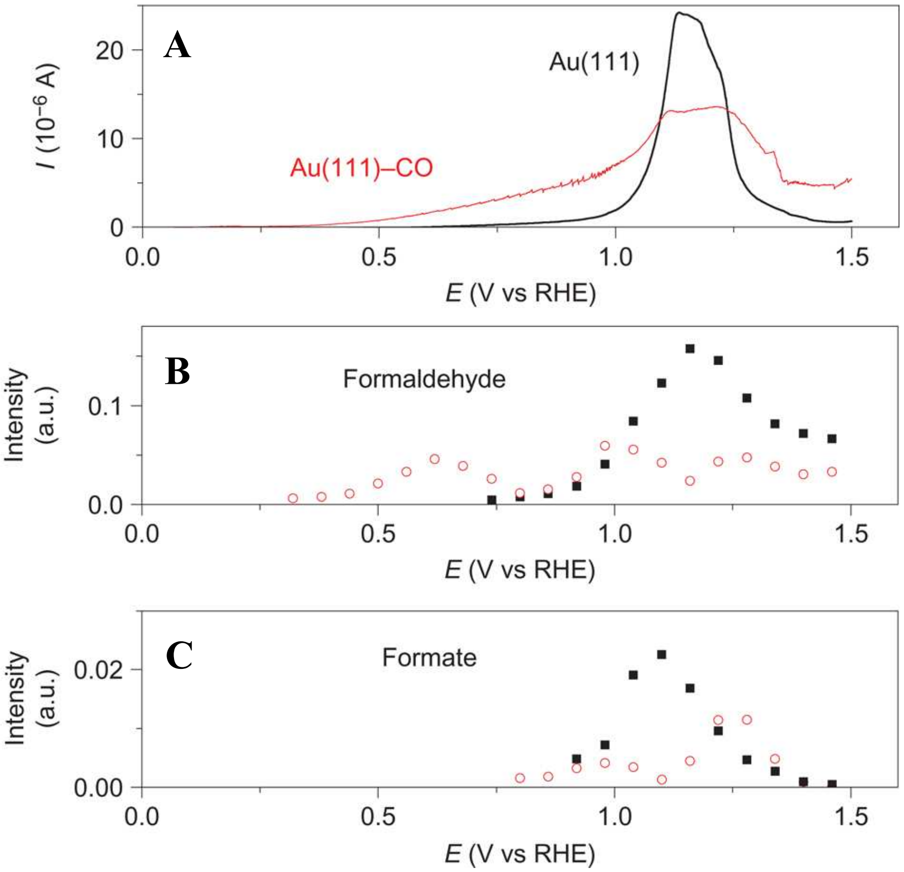
A
Au(111)
Au(111)–CO
I (10⁻⁶ A)
20
10
0
0.0
0.5
1.0
1.5
E (V vs RHE)
B
Formaldehyde
Intensity (a.u.)
0.1
0.0
C
Formate
0.02
0.00

Figure 5.

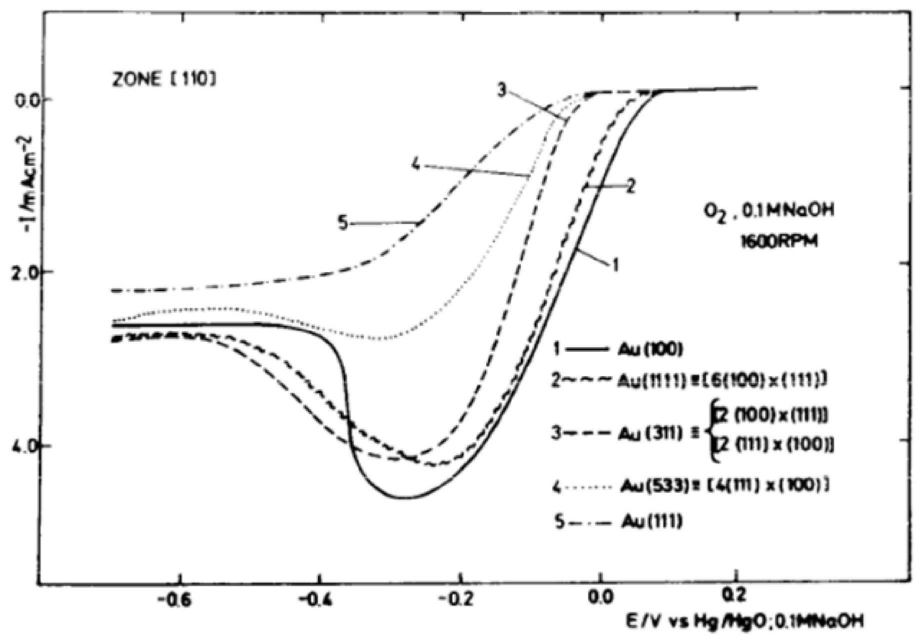
ZONE [110]
$-I$/mAcm^{-2}
0.0
2.0
4.0
O_2, 0.1MNaOH
1600RPM
1
2
3
4
5
1 —— Au(100)
2 - - - Au(1111) ≡ [6(100) x (111)]
3 - - - Au(311) ≡ {[2 (100) x (111)] / [2 (111) x (100)]}
4 ······ Au(533) ≡ [4(111) x (100)]
5 -·- Au(111)
-0.6
-0.4
-0.2
0.0
0.2
E/V vs Hg/HgO; 0.1MNaOH

Figure 6.

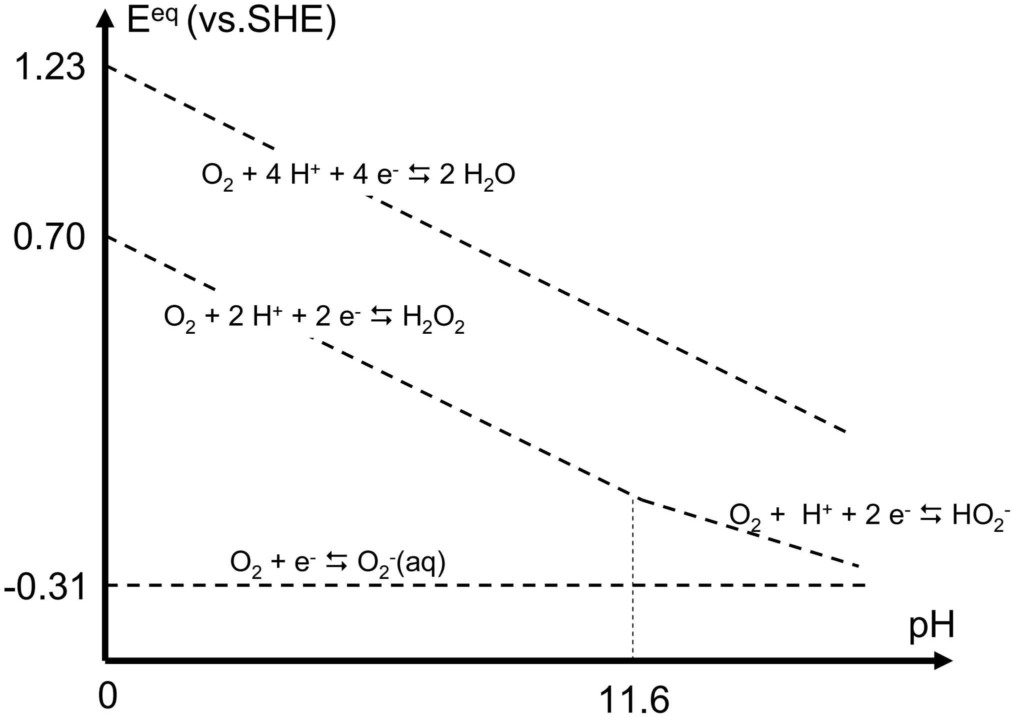
E^{eq} (vs.SHE)
1.23
0.70
-0.31
$O_2 + 4 H^+ + 4 e^- \leftrightarrows 2 H_2O$
$O_2 + 2 H^+ + 2 e^- \leftrightarrows H_2O_2$
$O_2 + H^+ + 2 e^- \leftrightarrows HO_2^-$
$O_2 + e^- \leftrightarrows O_2^-(aq)$
pH
0
11.6

Figure 7

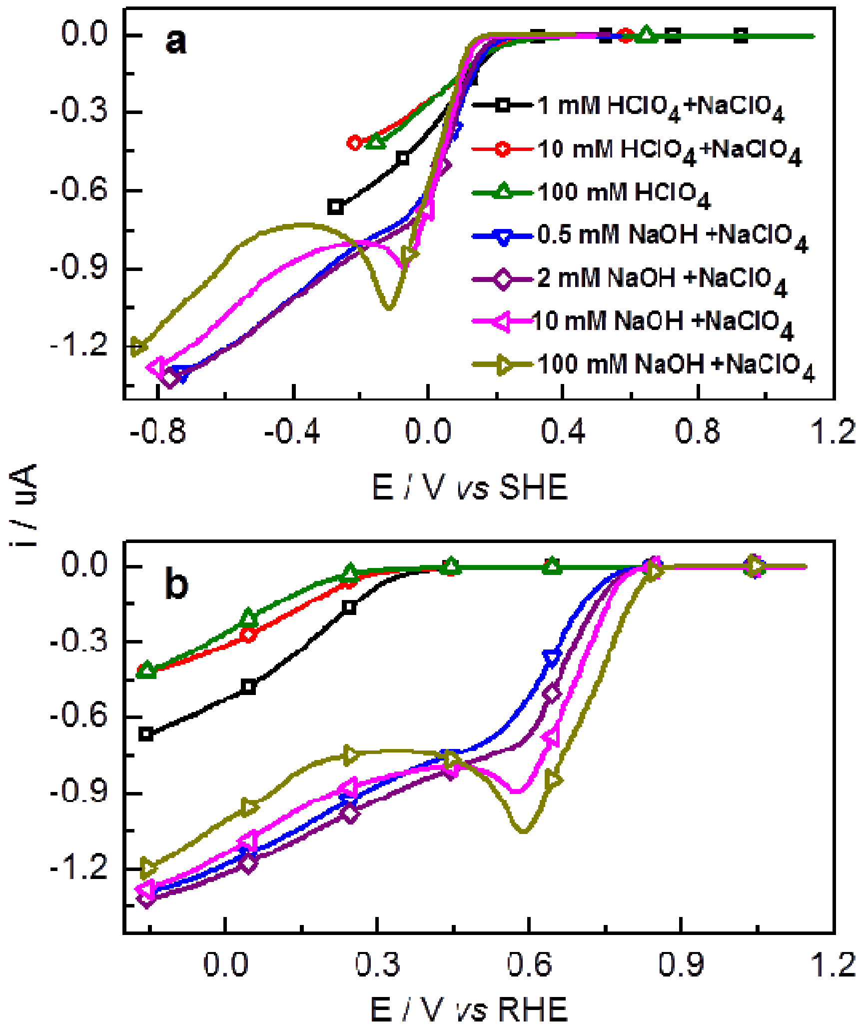
a
0.0
-0.3
-0.6
-0.9
-1.2
1 mM $HClO_4$+$NaClO_4$
10 mM $HClO_4$+$NaClO_4$
100 mM $HClO_4$
0.5 mM NaOH +$NaClO_4$
2 mM NaOH +$NaClO_4$
10 mM NaOH +$NaClO_4$
100 mM NaOH +$NaClO_4$
-0.8
-0.4
0.0
0.4
0.8
1.2
E / V vs SHE
i / uA
b
0.0
-0.3
-0.6
-0.9
-1.2
0.0
0.3
0.6
0.9
1.2
E / V vs RHE

Figure 8.

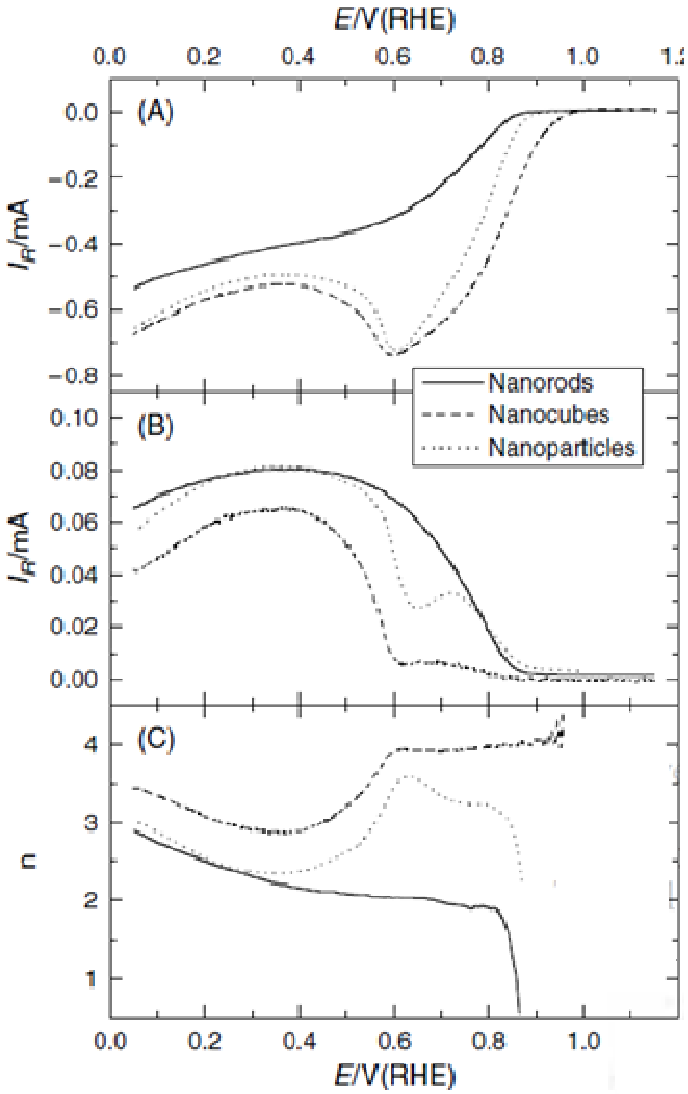
E/V(RHE)
0.0
0.2
0.4
0.6
0.8
1.0
1.2
(A)
I_R/mA
0.0
−0.2
−0.4
−0.6
−0.8
Nanorods
Nanocubes
Nanoparticles
(B)
I_R/mA
0.10
0.08
0.06
0.04
0.02
0.00
(C)
n
4
3
2
1
0.0
0.2
0.4
0.6
0.8
1.0
E/V(RHE)

Figure 9.

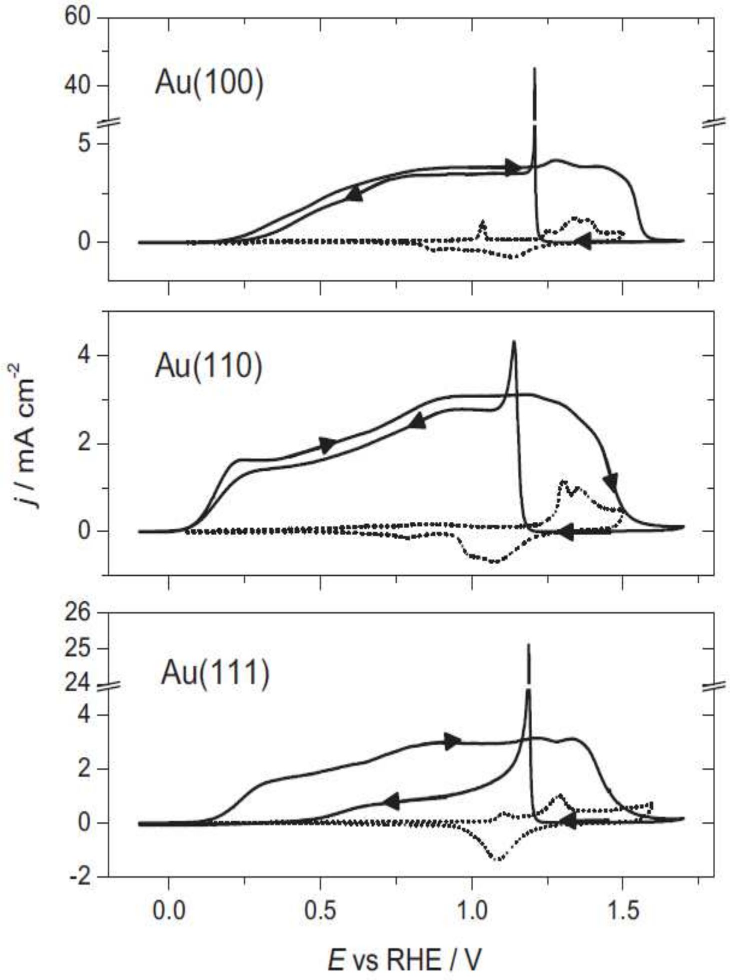
Au(100)
Au(110)
Au(111)
60
40
5
0
4
2
0
26
25
24
4
2
0
-2
j / mA cm^{-2}
0.0
0.5
1.0
1.5
E vs RHE / V

Figure 10.

References

(1) Tremiliosi-Filho, G.; Gonzalez, E. R.; Motheo, A. J.; Belgsir, E. M.; Leger, J. M.; Lamy, C. *Journal of Electroanalytical Chemistry* **1998**, *444*, 31.

(2) Sanchez, A.; Abbet, S.; Heiz, U.; Schneider, W. D.; Häkkinen, H.; Barnett, R. N.; Landman, U. *The Journal of Physical Chemistry A* **1999**, *103*, 9573.

(3) Rodriguez, P.; Kwon, Y.; Koper, M. T. M. *Nat Chem* **2012**, *4*, 177.

(4) Mirkin, M. V.; Yang, H.; Bard, A. J. *Journal of The Electrochemical Society* **1992**, *139*, 2212.

(5) Mavrikakis, M.; Stoltze, P.; Norskov, J. K. *Catalysis Letters* **2000**, *64*, 101.

(6) Lopez, N.; Janssens, T. V. W.; Clausen, B. S.; Xu, Y.; Mavrikakis, M.; Bligaard, T.; Nørskov, J. K. *Journal of Catalysis* **2004**, *223*, 232.

(7) Hutchings, G. J.; Haruta, M. *Applied Catalysis a-General* **2005**, *291*, 2.

(8) Haruta, M. *Nature* **2005**, *437*, 1098.

(9) Haruta, M. *Chemical record (New York, N.Y.)* **2003**, *3*, 75.

(10) Grisel, R.; Weststrate, K. J.; Gluhoi, A.; Nieuwenhuys, B. E. *Gold Bulletin* **2002**, *35*, 39.

(11) Carabineiro, S. A. C.; Nieuwenhuys, B. E. *Gold Bulletin* **2009**, *42*, 288.

(12) Baker, T. A.; Liu, X. Y.; Friend, C. M. *Physical Chemistry Chemical Physics* **2011**, *13*, 34.

(13) Takei, T.; Iguchi, N.; Haruta, M. *New Journal of Chemistry* **2011**, *35*, 2227.

(14) Hutchings, G. J.; Hall, M. S.; Carley, A. F.; Landon, P.; Solsona, B. E.; Kiely, C. J.; Herzing, A.; Makkee, M.; Moulijn, J. A.; Overweg, A.; Fierro-Gonzalez, J. C.; Guzman, J.; Gates, B. C. *Journal of Catalysis* **2006**, *242*, 71.

(15) Hutchings, G. J.; Brust, M.; Schmidbaur, H. *Chemical Society Reviews* **2008**, *37*, 1759.

(16) Haruta, M.; Tsubota, S.; Ueda, A.; Sakurai, H. *Studies in Surface Science and Catalysis* **1993**, *77*, 45.

(17) Haruta, M. *Cattech* **2002**, *6*, 102.

(18) Choudhary, T. V.; Goodman, D. W. *Applied Catalysis A: General* **2005**, *291*, 32.

(19) Haruta, M.; Yamada, N.; Kobayashi, T.; Iijima, S. *Journal of Catalysis* **1989**, *115*, 301.

(20) Liu, X.; Klust, A.; Madix, R. J.; Friend, C. M. *The Journal of Physical Chemistry C* **2007**, *111*, 3675.

(21) Liu, X.; Friend, C. M. *The Journal of Physical Chemistry C* **2010**, *114*, 5141.

(22) Landis, E. C.; Jensen, S. C.; Phillips, K. R.; Friend, C. M. *The Journal of Physical Chemistry C* **2012**, *116*, 21508.

(23) Hussain, A.; Ferre, D. C.; Gracia, J.; Nieuwenhuys, B. E.; Niemantsverdriet, J. W. *Surface Science* **2009**, *603*, 2734.

(24) Liu, X.; Friend, C. M. *Langmuir* **2010**, *26*, 16552.

(25) Ishida, T.; Kinoshita, N.; Okatsu, H.; Akita, T.; Takei, T.; Haruta, M. *Angewandte Chemie-International Edition* **2008**, *47*, 9265.

(26) Roberts Jr, J. L.; Sawyer, D. T. *Electrochimica Acta* **1965**, *10*, 989.

(27) Roberts Jr, J. L.; Sawyer, D. T. *Journal of Electroanalytical Chemistry (1959)* **1964**, *7*, 315.

(28) Saez, A.; Solla-Gullon, J.; Exposito, E.; Montiel, V.; Aldaz, A. *Electrochimica Acta* **2009**, *54*, 7071.

(29) Rodríguez, P.; Koverga, A. A.; Koper, M. T. M. *Angewandte Chemie International Edition* **2010**, *49*, 1241.

(30) Rodriguez, P.; Garcia-Araez, N.; Koverga, A.; Frank, S.; Koper, M. T. M. *Langmuir* **2010**, *26*, 12425.

(31) Rodriguez, P.; Garcia-Araez, N.; Koper, M. T. M. *Physical Chemistry Chemical Physics* **2010**, *12*, 9373.

(32) Rodriguez, P.; Feliu, J. M.; Koper, M. T. M. *Electrochemistry Communications* **2009**, *11*, 1105.

(33) Kwon, Y.; Schouten, K. J. P.; Koper, M. T. M. *Chemcatchem* **2011**, *3*, 1176.

(34) Blizanac, B. B.; Arenz, M.; Ross, P. N.; Marković, N. M. *J. Am. Chem. Soc.* **2004**, *126*, 10130.

(35) Plana, D.; Dryfe, R. A. W. *Electrochimica Acta* **2011**, *56*, 3835.

(36) Plana, D.; Rodriguez, P.; Koper, M. T. M.; Dryfe, R. A. W. *Electrochimica Acta* **2011**, *56*, 7637.

(37) Edens, G. J.; Hamelin, A.; Weaver, M. J. *The Journal of Physical Chemistry* **1996**, *100*, 2322.

(38) Cuesta, A.; López, N.; Gutiérrez, C. *Electrochimica Acta* **2003**, *48*, 2949.

(39) Kwon, Y.; Lai, S. C. S.; Rodriguez, P.; Koper, M. T. M. *J. Am. Chem. Soc.* **2011**, *133*, 6914.

(40) Adić, R. R.; Marković, N. M.; Vešović, V. B. *Journal of Electroanalytical Chemistry and Interfacial Electrochemistry* **1984**, *165*, 105.

(41) Marković, N. M.; Adić, R. R.; Vešović, V. B. *Journal of Electroanalytical Chemistry and Interfacial Electrochemistry* **1984**, *165*, 121.

(42) Schmidt, T. J.; Stamenkovic, V.; Arenz, M.; Markovic, N. M.; Ross Jr, P. N. *Electrochimica Acta* **2002**, *47*, 3765.

(43) Hayden, B. E.; Pletcher, D.; Suchsland, J.-P. *Angewandte Chemie-International Edition* **2007**, *46*, 3530.

(44) Hayden, B. E.; Pletcher, D.; Rendall, M. E.; Suchsland, J.-P. *J. Phys. Chem. C* **2007**, *111*, 17044.

(45) Gallagher, M. E.; Blizanac, B. B.; Lucas, C. A.; Ross, P. N.; Markovic, N. M. *Surface Science* **2005**, *582*, 215.

(46) Beltramo, G. L.; Shubina, T. E.; Koper, M. T. M. *ChemPhysChem* **2005**, *6*, 2597.

(47) Garcia, G.; Koper, M. T. M. *Physical Chemistry Chemical Physics* **2008**, *10*, 3802.

(48) Kunimatsu, K.; Aramata, A.; Nakajima, H.; Kita, H. *Journal of Electroanalytical Chemistry* **1986**, *207*, 293.

(49) Kita, H.; Nakajima, H.; Hayashi, K. *Journal of Electroanalytical Chemistry and Interfacial Electrochemistry* **1985**, *190*, 141.

(50) Rodriguez, P.; Plana, D.; Fermin, D. J.; Koper, M. T. M. *Journal of Catalysis* **2014**, *311*, 182.

(51) Antolini, E. *J. Power Sources* **2007**, *170*, 1.

(52) Vigier, F.; Coutanceau, C.; Perrard, A.; Belgsir, E. M.; Lamy, C. *Journal of Applied Electrochemistry* **2004**, *34*, 439.

(53) Rousseau, S.; Coutanceau, C.; Lamy, C.; Leger, J. M. *J. Power Sources* **2006**, *158*, 18.

(54) Lamy, C.; Rousseau, S.; Belgsir, E. M.; Coutanceau, C.; Leger, J. M. *Electrochimica Acta* **2004**, *49*, 3901.

(55) Lamy, C.; Belgsir, E. M.; Leger, J. M. *Journal of Applied Electrochemistry* **2001**, *31*, 799.

(56) Lai, S. C. S.; Kleijn, S. E. F.; Ozturk, F. T. Z.; Vellinga, V. C. v. R.; Koning, J.; Rodriguez, P.; Koper, M. T. M. *Catalysis Today* **2010**, *154*, 92.

(57) Jeffery, D. Z.; Camara, G. A. *Electrochemistry Communications* **2010**, *12*, 1129.

(58) Gomes, J.; Tremiliosi-Filho, G. *Electrocatalysis* **2011**, *2*, 96.

(59) A. Larew, L.; Johnson, D. C. *Journal of Electroanalytical Chemistry and Interfacial Electrochemistry* **1989**, *262*, 167.

(60) Casella, I. G.; Gatta, M.; Contursi, M. *Journal of Electroanalytical Chemistry* **2004**, *561*, 103.

(61) Wang, G.; He, X.; Wang, L.; Gu, A.; Huang, Y.; Fang, B.; Geng, B.; Zhang, X. *Microchim Acta* **2013**, *180*, 161.

(62) Compton, K. E. T. R. G. *Int. J. Electrochem. Sci* **2010**, *5*.

(63) Xia, Y.; Huang, W.; Zheng, J.; Niu, Z.; Li, Z. *Biosensors and Bioelectronics* **2011**, *26*, 3555.

(64) Kokoh, K. B.; Léger, J. M.; Beden, B.; Lamy, C. *Electrochimica Acta* **1992**, *37*, 1333.

(65) Rao, M. L. B.; Drake, R. F. *Journal of The Electrochemical Society* **1969**, *116*, 334.

(66) Kokoh, K. B.; Léger, J. M.; Beden, B.; Huser, H.; Lamy, C. *Electrochimica Acta* **1992**, *37*, 1909.

(67) Governo, A. T.; Proença, L.; Parpot, P.; Lopes, M. I. S.; Fonseca, I. T. E. *Electrochimica Acta* **2004**, *49*, 1535.

(68) Adžić, R. R.; Avramov-Ivić, M. *Journal of Catalysis* **1986**, *101*, 532.

(69) Borkowska, Z.; Tymosiak-Zielinska, A.; Shul, G. *Electrochimica Acta* **2004**, *49*, 1209.

(70) Beyhan, S.; Uosaki, K.; Feliu, J. M.; Herrero, E. *Journal of Electroanalytical Chemistry* **2013**, *707*, 89.

(71) Tripković, A. V.; Popović, K. D.; Momčilović, J. D.; Draić, D. M. *Journal of Electroanalytical Chemistry* **1996**, *418*, 9.

(72) Koverga, A. A.; Frank, S.; Koper, M. T. M. *Electrochimica Acta* **2013**, *101*, 244.

(73) Hernandez, J.; Solla-Gullon, J.; Herrero, E.; Aldaz, A.; Feliu, J. M. *Electrochimica Acta* **2006**, *52*, 1662.

(74) Yan, S.; Zhang, S.; Lin, Y.; Liu, G. *The Journal of Physical Chemistry C* **2011**, *115*, 6986.

(75) Wang, D.; Huang, J.; Liu, Y.; Han, X.; You, T. *J Nanopart Res* **2011**, *13*, 157.

(76) Jena, B. K.; Raj, C. R. *Langmuir* **2007**, *23*, 4064.

(77) Feng, J.-J.; Li, A.-Q.; Lei, Z.; Wang, A.-J. *ACS Applied Materials & Interfaces* **2012**, *4*, 2570.

(78) Qiao, Y.; Chen, H.; Lin, Y.; Huang, J. *Langmuir* **2011**, *27*, 11090.

(79) Ballarin, B.; Cassani, M. C.; Gazzano, M.; Solinas, G. *Electrochimica Acta* **2010**, *56*, 676.

(80) Ballarin, B.; Cassani, M. C.; Maccato, C.; Gasparotto, A. *Nanotechnology* **2011**, *22*, 275711.

(81) Ketchie, W. C.; Fang, Y.-L.; Wong, M. S.; Murayama, M.; Davis, R. J. *Journal of Catalysis* **2007**, *250*, 94.

(82) Zope, B. N.; Hibbitts, D. D.; Neurock, M.; Davis, R. J. *Science* **2010**, *330*, 74.

(83) Comotti, M.; Della Pina, C.; Falletta, E.; Rossi, M. *Advanced Synthesis & Catalysis* **2006**, *348*, 313.

(84) Nijhuis, T. A.; Weckhuysen, B. M. *Catalysis Today* **2006**, *117*, 84.

(85) Kwon, Y.; Raaijman, S. J.; Koper, M. T. M. *Chemcatchem* **2014**, *6*, 79.

(86) Guerin, S.; Hayden, B. E.; Pletcher, D.; Rendall, M. E.; Suchsland, J.-P. *Journal of Combinatorial Chemistry* **2006**, *8*, 679.

(87) Zurilla, R. W.; Sen, R. K.; Yeager, E. *Journal of The Electrochemical Society* **1978**, *125*, 1103.

(88) Hernández, J.; Solla-Gullón, J.; Herrero, E.; Aldaz, A.; Feliu, J. M. *The Journal of Physical Chemistry C* **2007**, *111*, 14078.

(89) Markovic, N. M.; Schmidt, T. J.; Stamenkovic, V.; Ross, P. N. *Fuel Cells* **2001**, *1*, 105.

(90) Blizanac, B. B.; Lucas, C. A.; Gallagher, M. E.; Arenz, M.; Ross, P. N.; Marković, N. M. *The Journal of Physical Chemistry B* **2003**, *108*, 625.

(91) Adžić, R. R.; Strbac, S.; Anastasijević, N. *Materials Chemistry and Physics* **1989**, *22*, 349.

(92) Štrbac, S.; Anastasijević, N. A.; Adžić, R. R. *Journal of Electroanalytical Chemistry* **1992**, *323*, 179.

(93) Damjanovic, A.; Genshaw, M. A.; Bockris, J. O. M. *Journal of Electroanalytical Chemistry and Interfacial Electrochemistry* **1967**, *15*, 173.

(94) Adžić, R. R.; Marković, N. M. *Journal of Electroanalytical Chemistry and Interfacial Electrochemistry* **1982**, *138*, 443.

(95) Koper, M. T. M. *Chem. Sci.* **2013**, *4*, 2710.

(96) CHEN QuanJun, Z. Y., LIAO LingWen, KANG Jing, CHEN YanXia *Scientia Sinica Chimica* **2011**, *41*, 1777.

(97) Quaino, P.; Luque, N. B.; Nazmutdinov, R.; Santos, E.; Schmickler, W. *Angewandte Chemie International Edition* **2012**, *51*, 12997.

(98) Viswanathan, V.; Hansen, H. A.; Rossmeisl, J.; Norskov, J. K. *ACS Catalysis* **2012**, *2*, 1654.

(99) Štrbac, S.; Anastasijević, N. A.; Adžić, R. R. *Electrochimica Acta* **1994**, *39*, 983.

(100) Kim, J.; Gewirth, A. A. *Journal of Physical Chemistry B* **2006**, *110*, 2565.

(101) Vassilev, P.; Koper, M. T. M. *J. Phys. Chem. C* **2007**, *111*, 2607.

(102) Koper, M. T. M. *Nanoscale* **2011**, *3*, 2054.

(103) Li, H.; Calle-Vallejo, F.; Kolb, M. J.; Kwon, Y.; Li, Y.; Koper, M. T. M. *J. Am. Chem. Soc.* **2013**, *135*, 14329.

(104) Hernández, J.; Herrero, E.; Solla-Gullón, J.; Vidal-Iglesias, F. J.; Feliu, J. M.; Aldaz, A. 2005; Vol. PV 2005-11, p 200.

(105) Hernández, J.; Solla-Gullón, J.; Herrero, E. *Journal of Electroanalytical Chemistry* **2004**, *574*, 185.

(106) Hernández, J.; Solla-Gullón, J.; Herrero, E.; Feliu, J. M.; Aldaz, A. *Journal of Nanoscience and Nanotechnology* **2009**, *9*, 2256.

(107) Brülle, T.; Ju, W.; Niedermayr, P.; Denisenko, A.; Paschos, O.; Schneider, O.; Stimming, U. *Molecules* **2011**, *16*, 10059.

(108) Chatenet, M.; Micoud, F.; Roche, I.; Chainet, E. *Electrochimica Acta* **2006**, *51*, 5459.

(109) Concha, B. M.; Chatenet, M.; Coutanceau, C.; Hahn, F. *Electrochemistry Communications* **2009**, *11*, 223.

(110) Santos, D. M. F.; Sequeira, C. A. C. *Journal of The Electrochemical Society* **2009**, *156*, F67.

(111) Molina Concha, B.; Chatenet, M. *Electrochimica Acta* **2009**, *54*, 6119.

(112) Gyenge, E.; Atwan, M.; Northwood, D. *Journal of The Electrochemical Society* **2006**, *153*, A150.

(113) Molina Concha, B.; Chatenet, M. *Electrochimica Acta* **2009**, *54*, 6130.

(114) Atwan, M. H.; Macdonald, C. L. B.; Northwood, D. O.; Gyenge, E. L. *J. Power Sources* **2006**, *158*, 36.

(115) Chatenet, M.; Lima, F. H. B.; Ticianelli, E. A. *Journal of The Electrochemical Society* **2010**, *157*, B697.

(116) Hori, Y. In *Modern Aspects of Electrochemistry*; Vayenas, C., White, R., Gamboa-Aldeco, M., Eds.; Springer New York: 2008; Vol. 42, p 89.

(117) Koper, M. T. M. *Journal of Electroanalytical Chemistry* **2011**, *660*, 254.

(118) Chen, Y.; Li, C. W.; Kanan, M. W. *J. Am. Chem. Soc.* **2012**, *134*, 19969.

(119) Zhu, W.; Michalsky, R.; Metin, Ö.; Lv, H.; Guo, S.; Wright, C. J.; Sun, X.; Peterson, A. A.; Sun, S. *J. Am. Chem. Soc.* **2013**, *135*, 16833.

(120) Noda, H.; Ikeda, S.; Yamamoto, A.; Einaga, H.; Ito, K. *Bulletin of the Chemical Society of Japan* **1995**, *68*, 1889.